ACS Sustainable Chemistry & Engineering

Research Article

pubs.acs.org/journal/ascecg

Gel-Like Dispersions of HMDI-Cross-Linked Lignocellulosic Materials in Castor Oil: Toward Completely Renewable Lubricating Grease Formulations

R. Gallego,[†] J. F. Arteaga,[†,‡] C. Valencia,[†,§] M. J. Díaz,[†,§] and J. M. Franco*[,†,§]

[†]Departamento de Ingeniería Química, Química Física y Química Orgánica, Campus de "El Carmen", Universidad de Huelva, Campus de Excelencia Internacional Agroalimentario, ceiA3, 21071 Huelva, Spain

[‡]CIQSO − Center for Research in Sustainable Chemistry, Universidad de Huelva, 21071 Huelva, Spain

[§]Pro[2]TecS − Chemical Process and Product Technology Research Center, Universidad de Huelva, 21071 Huelva, Spain

ABSTRACT: In this work, several lignocellulose pulps from different origins and/or submitted to different treatments were cross-linked with hexamethylene diisocyanate (HMDI) and further dispersed in castor oil in order to obtain gel-like formulations based on renewable resources, which can be potentially applicable as semisolid lubricants. The rheological and tribological properties attained as well as physical and mechanical stability were suitable to consider these gel-like dispersions as efficient alternatives to traditional lubricating greases. The rheological behavior was evaluated by means of both small-amplitude oscillatory shear tests (SAOS) and viscous flow measurements, at different temperatures. The HMDI/cellulose pulp weight ratio applied in the cross-linking reaction can be used to modify and modulate the consistency and the values of rheological functions of these gel-like dispersions. However, the rheological behavior is not qualitatively affected by the amount of HMDI used as coupling agent. The thermo-rheological response evidences a softening temperature of around 100 °C. Mechanical stability of HMDI-cross-linked lignocellulose-based oleogels, evaluated as the loss of consistency after submitting the sample to a working test, was significantly improved respecting the non-cross-linked lignocellulose gel-like dispersion. Microstructural morphology was examined using atomic force microscopy (AFM) and consists of long and entangled fibers, extremely similar to that found in lithium greases. Moreover, friction coefficient and resulting wear mark diameters obtained in a ball-on-disc contact lubricated with these eco-friendly formulations were, in most cases, comparable to that obtained with commercial lubricating greases. Therefore, HMDI-cross-linked lignocellulose materials are proposed as effective and promising eco-friendly thickener agents in vegetable oils.

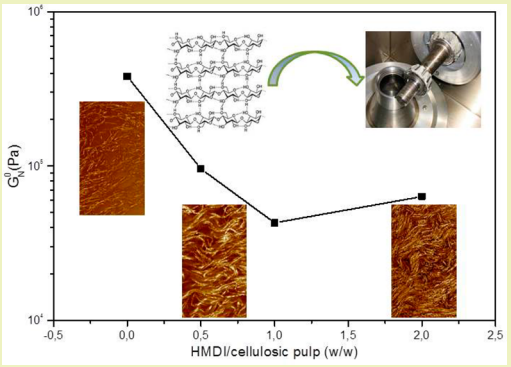

KEYWORDS: *Castor oil, Isocyanate, Lignocellulose, Lubricating grease, Oleogel, Rheology*

INTRODUCTION

In the frame of environmental protection, different strategies for the replacement of nonrenewable raw materials by renewable resources are targeted to reduce the impact that process technologies and products of different industrial sectors cause in the environment. In this sense, the concept of biorefinery arises as an integrated industrial metabolism able to produce chemical intermediates, end-use materials, and energy based on the principles of green chemistry and engineering.[1] One example of the industrial sector with particular environmental awareness and capacity to exploit different agro-resources and vegetable-derived products is the lubricant industry.[2−5] A great number of research work analyzing the lubricant properties of different vegetable oils and derivatives resulting from chemical modifications have been reported in the last years. Among them, castor oil is considered one of the most interesting alternative base oils, especially due to its high viscosity and good performance characteristics at low temperatures.[6−8] Moreover, despite the fact that additives are usually included in small proportions, special attention has been also paid on the development of green multifunctional additives for lubricant formulations in order to improve specific properties of vegetable oil-derived base oils, such as viscosity index, pour point, thermo-oxidative stability, lubricity, antiwear, and detergent dispersant capacity.[9−15] Therefore, a wide range of alternatives to design efficient liquid lubricant products completely based on renewable resources are available in the existing literature. A major complexity involves the formulation of semisolid lubricants, i.e., lubricating greases. In these formulations, another key component needs to be added to impart the desired rheological properties and gel-like characteristics, the so-called thickener agent. The substitution of traditional thickener agents in lubricating greases, such as metallic soaps and polyureas, by others derived from renewable

Received: May 4, 2015
Revised: July 22, 2015
Published: July 24, 2015

DOI: 10.1021/acssuschemeng.5b00389
ACS Sustainable Chem. Eng. 2015, 3, 2130−2141

Table 1. Composition and Intrinsic Viscosity of Mercerized Lignocellulose Samples

thickener	α-cellulose[a] (% w/w)	hemicellulose[b] (% w/w)	lignin[c] (% w/w)	intrinsic viscosity[d] (cm^3/g)
Pinus radiata (Kraft cooking)	82.6 ± 3.3	10.2 ± 1.1	5.7 ± 0.9	742
Eucalyptus globulus (semimechanical cooking)	59.7 ± 2.5	17.3 ± 1.6	22.1 ± 2.4	691
Eucalyptus globulus (Kraft cooking-commercial grade)	88.7 ± 3.6	9.1 ± 0.8	0.4 ± 0.1	584

[a]According to Tappi T-20-05-61. [b]According to ref 43. [c]According to Tappi T-222. [d]According to Tappi T-230.

Table 2. Proportions of Lignocellulose Pulp, Hexamethylene Diisocyanate (HMDI), Triethylamine (Et_3N), and Toluene Applied in the Cross-Linking Reaction and Codes of Each Sample

pulp origin	mercerized pulp (g)	HMDI (g)	Et_3N (g)	toluene (ml)	HMDI/mercerized pulp (w/w)	thickener code	oleogel code
Pinus radiata (Kraft cooking)	5	5	10	300	1	PK	GPK
Eucalyptus globulus (semimechanical cooking)					1	ES	GES
Eucalyptus globulus (Kraft cooking-commercial grade)					1	EK1	GEK1
		10	20		2	EK2	GEK2
		2.5	5		0.5	EK0.5	GEK0.5
	only mercerized				0	EK0	GEK0

resources is still a nontotally solved issue, mainly due to the high technical efficiency achieved with the traditional ones. Apart from providing suitable rheological characteristics, alternative eco-friendly thickeners need to impart additional properties like thermal and mechanical stability. This means that gel-like properties must be preserved at temperatures of around 100−150 °C and recovered after working in a lubricated contact. Taking up the biorefinery concept, some attempts to use lignocellulosic materials to thicken vegetable oils have been made in previous investigations.[16−18] The rheological functions of gel-like dispersions of several cellulosic pulps were found to increase with the polymerization degree and slightly decrease with lignin content. However, some weaknesses mainly regarding physical and mechanical stabilities were pointed out. In most cases, the mechanical resistance, determined as increment in penetration (or loss of consistency) after performing standardized shear rolling tests, was higher than 30 mm/10, which in principle should be reduced below 10 mm/10. In addition to this, a fraction of ethylated or methylated derivatives was needed to be used to improve physical stability, increasing the affinity by the oil medium and thus avoiding significant phase separation.

As may be deduced from several reviews,[19,20] the use of lignocellulosic materials to develop biodegradable composites has exponentially increased in the past decade. In many cases, lignocellulosic fibers were used as fillers to reinforce some tensile and flexural properties by just applying relatively simple thermal treatments.[21−25] However, different chemical modifications and/or additivation of lignocellulosic fibers have been performed to enhance specific properties.[20,26,27] Most reported chemical modification of lignocellulosic materials is the condensation reaction with isocyanates yielding biobased polyurethanes with different properties and applications as fillers in composite materials, foams, films, adhesives, etc.[28,29] Cross-linking reactions with diisocyanate compounds result in materials with improved mechanical and thermal resistance,[30−34] but also they may be directed to increase the hydrophobicity of cellulosic fibers,[35−37] favor the dispersion in organic solvents,[38] or contribute to a network formation[39] thus obtaining macro- or nanoporous matrixes.[40,41] Taking into account these considerations, in this work several lignocellulose pulps from different origin and/or submitted to different treatments were cross-linked with HMDI in order to induce the formation of a physically and mechanically stable three-dimensional network with enhanced hydrophobic interactions once dispersed in castor oil. The rheological properties and microstructure as well as lubricant performance of the different products were then evaluated.

EXPERIMENTAL SECTION

Materials. Castor oil (211 cSt at 40 °C, Guinama, Spain) was selected as a biodegradable lubricating base oil. Different lignocellulosic materials were submitted to a cross-linking reaction using 1,6-hexamethylene diisocyanate (HMDI) purum grade (≥98.0%), from Sigma-Aldrich, as a coupling agent. A commercial grade Kraft cellulose pulp from *Eucalyptus globulus* was kindly supplied by ENCE, S.A. (Huelva factory, Spain). Moreover, other cellulose pulps were produced in the laboratory from *Pinus radiata* and *Eucalyptus globulus* by applying classical Kraft cooking with an associate H factor of 940 or a semimechanical treatment, respectively. Kraft and semimechanical cooking details can be found elsewhere.[16] All other common reagents and solvents employed were purchased from Sigma-Aldrich.

Cross-Linking Reaction of Lignocellulosic Pulps. The cross-linking reaction was basically carried out following the protocol described to functionalize methyl cellulose.[42] Previously, a mercerization treatment was applied on lignocellulosic starting materials in order to deshield and make more accessible the groups susceptible to chemical modification. Typically, 5 g of pulp was soaked in 125 g of 50% NaOH solution under gentle agitation during 3 h at room temperature, and then the resulting pulp was filtered and pressed to achieve a pulp/alkali ratio around 1/9 w/w. Finally, the product was washed twice with water and acetone. Intrinsic viscosity values, estimated using the Tappi T-230 standard method, and average composition determined according to Wise et al.[43] and Tappi methods of mercerized lignocellulose samples are shown in Table 1, whereas the characterization of original cellulosic pulps can be found elsewhere.[16] Afterward, mercerized pulp was added to a round bottomed flask with toluene while stirring at room temperature to create a suspension, and then, triethylamine (Et_3N) and HMDI were also added to the system in different proportions (see Table 2), the latter added dropwise. The solution was vigorously stirred at room temperature during 24 h. Finally, the mixture was filtered, resulting a white paste.

Preparation of Gel-Like Dispersions. HMDI-cross-linked lignocellulosic materials were dispersed in castor oil using a batch reactor (500 mL) and a controlled-rotational speed mixing device RW 20 (Ika), equipped with an anchor impeller. Lignocellulosic materials were slowly added to the oil under agitation (70 rpm) which was maintained for 24 h at room temperature. The dispersion was then homogenized with an Ultra-Turrax T50 (Ika) rotor-stator turbine, at

DOI: 10.1021/acssuschemeng.5b00389
ACS Sustainable Chem. Eng. 2015, 3, 2130−2141

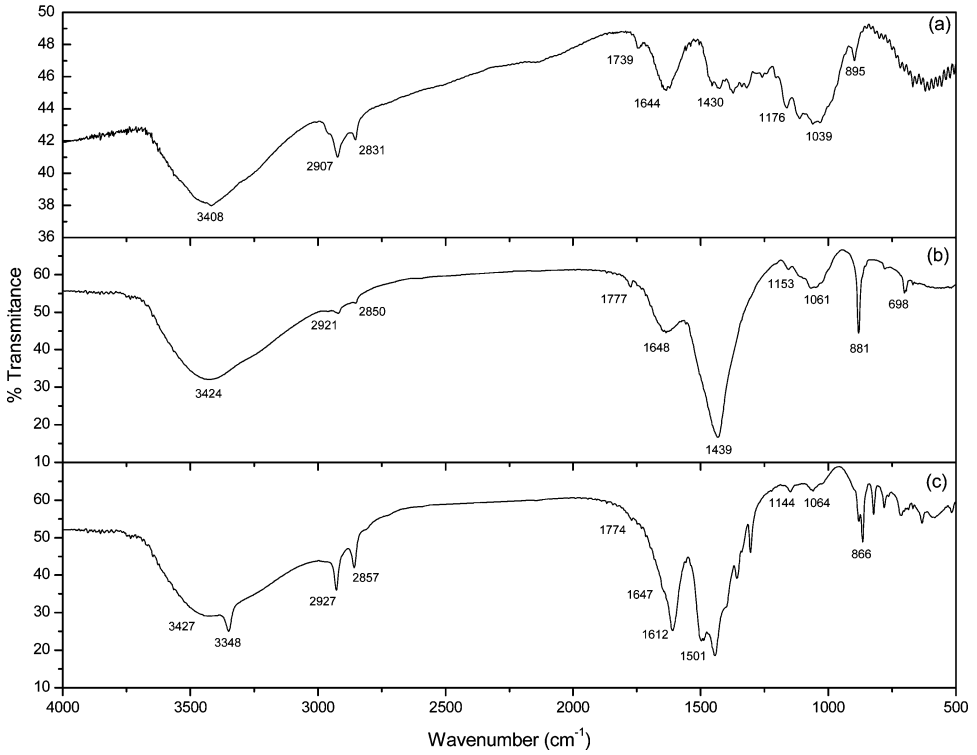

Figure 1. FTIR spectra for different lignocellulosic materials: (a) original commercial grade Kraft pulp, (b) mercerized pulp (sample EK0), and (c) HMDI-cross-linked lignocellulosic material (sample EK2).

8800 rpm during 5 min, resulting in homogeneous oleogels. Concentration of HMDI-cross-linked lignocellulose pulp was fixed at 7% w/w. A dispersion of the nonchemically modified but mercerized commercial grade Kraft cellulose pulp in castor oil, at the same concentration, was also prepared for the sake of comparison. Codes applied to identify gel-like dispersions and corresponding lignocellulosic materials are collected in Table 2.

Fourier Transform Infrared Spectroscopy (FTIR). FTIR spectra were obtained with a Digilab FTS3500ARX (Varian) apparatus. Lignocellulose pulp samples were prepared as KBr pellets, and the set was placed into an appropriate sample holder. The spectra were obtained in a wavenumber range of 400−4000 cm^{-1}, at 4 cm^{-1} resolution, in the transmission mode.

Thermogravimetric Analysis (TGA). Measurements of mass loss versus temperature were carried out by using a thermogravimetric analyzer, model Q-50 (TA Instrument Waters, USA), under N_2 purge. The sample (5−10 mg) was placed on a platinum pan and heated from 30 to 600 °C, at 10 °C/min.

Atomic Force Microscopy. Morphological characterization of lignocellulose gel-like dispersions in castor oil was made by means of atomic force microscopy (AFM), with a multimode apparatus connected to a Nanoscope-IV scanning probe microscope controller (Digital Instruments, Veeco Metrology Group Inc., USA). All images were acquired in the tapping mode, using Veeco Nanoprobe tips, in phase imaging, where the cantilever oscillates at its resonant frequency. The amplitude was used as a feedback signal. Samples were not submitted to any physical modification or partial oil extraction but previously heated at around 100−110 °C by placing the AFM sample holder in an external heating plate for 20−30 s and, then, cooled down to room temperature to obtain smooth film surfaces.

Rheological Characterization. Rheological characterization of gel-like dispersions was carried out in a Physica MCR-501 rheometer (Anton Paar, Austria) equipped with a Peltier temperature controller, using a plate−plate geometry (25 mm diameter, 1 mm gap). Small-amplitude oscillatory shear (SAOS) tests were performed inside the linear viscoelastic region, in a frequency range of 0.03−100 rad/s. Viscous flow tests were performed by applying a stepped shear rate ramp (5 min per point) in a shear rate range of 10^{-2}−10^{2} s^{-1}, using a plate−plate geometry with grooved surfaces to overcome wall slip phenomena usually observed in lubricating greases.[44] Rheological measurements were obtained at different temperatures comprised between 5 and 150 °C. At least two replicates were performed on fresh samples.

Penetration and Mechanical Stability Tests. Penetration indexes were determined according to the ASTM D 1403 standard on fresh gel-like dispersions samples, by using a Seta Universal penetrometer, model 17000-2, with one-quarter cone geometry (Stanhope-Seta, UK). The one-quarter scale penetration values were converted into equivalent full-scale cone penetration values, according to the ASTM D-217 standard. HMDI-cross-linked lignocellulose gel-like dispersions in castor oil were worked on during 2 h in a Roll Stability Tester, model 19400-3 (Stanhope-Seta, UK), according to the ASTM D 1831 standard, and penetration measurements were performed, once again, immediately after this rolling test. The mechanical stability of gel-like dispersions studied was then estimated as the difference between worked and unworked penetration values.[45] At least three replicates of penetration measurements were performed.

Tribological Tests. Tribological tests were carried out in a tribology measuring cell coupled with a Physica MCR-501 rheometer. The tribological cell deals with a 1/2″ diameter steel ball (1.4301 grade 100) rotating on three 45° inclined steel plates (1.4301). The stationary friction coefficient was obtained by applying a normal force of 20 N, resulting a maximum contact Hertzian pressure of ≈1.72 GPa and setting a constant rotational speed of 10 rpm for 10 min. At least, five replicates of each test were performed on fresh samples at room temperature (25 °C). Resulting wear marks on the steel plates were examined using a FEI environmental scanning electronic microscope model Quanta 200. For the sake of comparison, tribological tests were also performed under the same conditions on two commercial lubricating greases, a typical lithium grease (Castrol Optipit, Germany) and a semibiodegradable one based on vegetable oil and a calcium thickener (Verkol, Spain).

DOI: 10.1021/acssuschemeng.5b00389
ACS Sustainable Chem. Eng. 2015, 3, 2130−2141

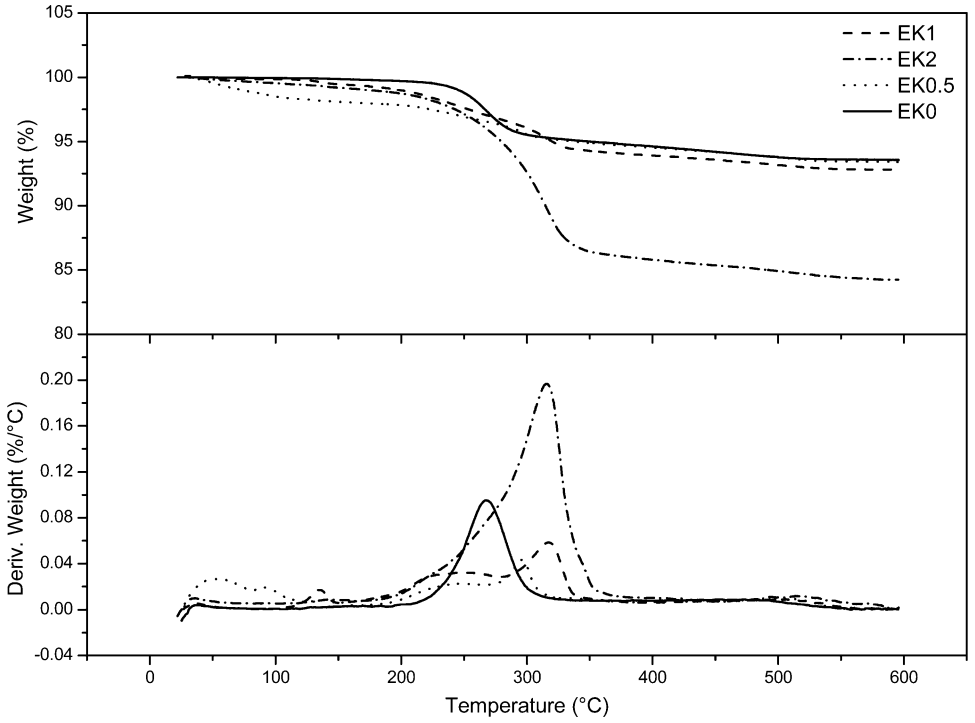

Figure 2. Thermal degradation curves, under inert atmosphere, for HMDI-cross-linked lignocellulosic materials, as a function of HMDI/cellulose pulp weight ratio. (a) weight loss curve and (b) derivative curve.

RESULTS AND DISCUSSION

Characterization of HMDI-Cross-Linked Lignocellulosic Materials. The FTIR technique was used to evaluate the chemical modification of the different cellulose pulps after mercerization with NaOH and further cross-linking with HMDI. Figure 1 shows the FTIR spectra of original commercial grade Kraft cellulose pulp (EK), the corresponding mercerized sample (EK0), and a selected HMDI-modified sample (EK2). The main differences between the spectra of the mercerized sample (Figure 1b) and original Kraft cellulose pulp (Figure 1a) were detected in the wavenumber ranges of 3600−2800 cm^{-1} and 1400−500 cm^{-1}. A modification and displacement in transmittance intensity of the bands at 2907 and 2831 cm^{-1}, respectively, assigned to C−H asymmetrical and symmetrical stretching vibrations of methylene groups, can be detected. The ratio of these absorption intensities is lower in the spectrum of the mercerized sample than that observed for the original lignocellulose pulp. Another important aspect of the mercerized sample infrared spectrum is the alteration in the shape of the band between 3700 and 2800 cm^{-1}, with a maximum around 3424 cm^{-1} assigned to −OH stretching absorptions. The peak located at 1739 cm^{-1} in EK and 1777 cm^{-1} in EK0 was attributed to C═O stretching of the acetyl group in hemicellulose.[46] However, the region from 1500 to 500 cm^{-1} is particularly sensitive to structural changes such as the increase or decrease in the degree of order or any alteration of hydrogen bonding occurred during mercerization, as well as to the kind of cellulosic derivative.[47,48] The mercerized sample IR spectrum in this region is characteristic of an amorphous pattern. An alteration of the crystalline organization leads to a significant simplification of the spectrum yielding a reduction in intensity or even disappearance of the characteristic bands attributable to crystalline domains.[49] Thus, the absorption bands in the 1400−881 cm^{-1} region are absent or strongly reduced in intensity, and only small bands at 1153 and 1061 cm^{-1} assigned to asymmetric C−O−C bridge stretching and C−O stretching, respectively, are observed. In addition to this, the absorption band at 1439 cm^{-1}, assigned to symmetric CH_2 bending vibration, increases. The absorption band at 881 cm^{-1}, assigned to C−O−C stretching of β-glycosidic linkages between the monosaccharides, is designed as an "amorphous" absorption band; an increase in its intensity occurring in the amorphous sample can be detected in Figure 1b, as previously described by Ciolacu et al.[49] Moreover, the C−OH bending peak is observed at 698 cm^{-1}. Finally, the HMDI modification (Figure 1c) can be confirmed by monitoring the shift of the bands at 2921 and 2850 cm^{-1}, assigned to the C−H stretching vibration, to higher wavenumber values and the increase in intensity of these bands. Moreover, a peak related to stretching of the N−H bond in the urethane group appears at 3348 cm^{-1}. However, new peaks at 1647, 1612, and 1501 cm^{-1} corresponding to C═O stretching, − C−N stretching, and N−H deformation of urethane linkages, respectively, can be observed. The absence of the signal at 2270 cm^{-1} corresponding to free isocyanate groups confirms that the cross-linking reaction using HMDI as coupling agent was almost completed, even in the sample EK2, containing the higher amount of HMDI.

Figure 2 shows the respective TGA and DTG curves of cellulose pulp derivatives modified to different extents with HMDI. According to this figure, slight differences in thermal decomposition profiles can be distinguished. A small weight loss for several samples occurs between 50 and 100 °C, which is attributed to the removal of absorbed water in cellulose pulp,[50] followed by some weight loss at around 120−140 °C corresponding to the thermal degradation of urethane segments.[42] After that, the thermal behavior of cellulose derivatives mainly consists of the linear cellulose skeleton degradation at ~300 °C.[51] In this stage, the breaking of glycosidic linkages reduces the polymerization degree leading to the formation of

DOI: 10.1021/acssuschemeng.5b00389
ACS Sustainable Chem. Eng. 2015, 3, 2130−2141

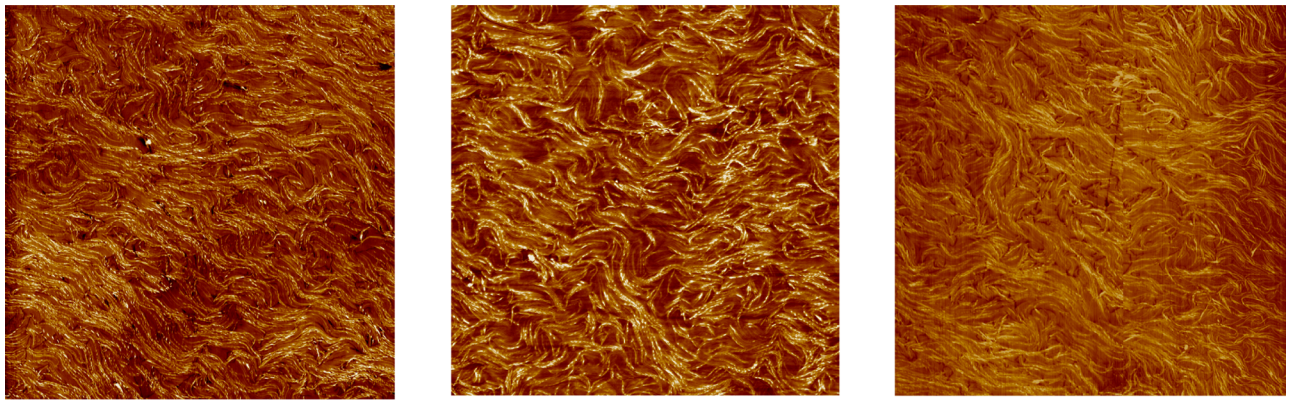

Figure 3. AFM micrographs (window size 20 μm) for selected HMDI-cross-linked lignocellulose gel-like dispersions: (a) GPK; (b) GEK1; (c) GES.

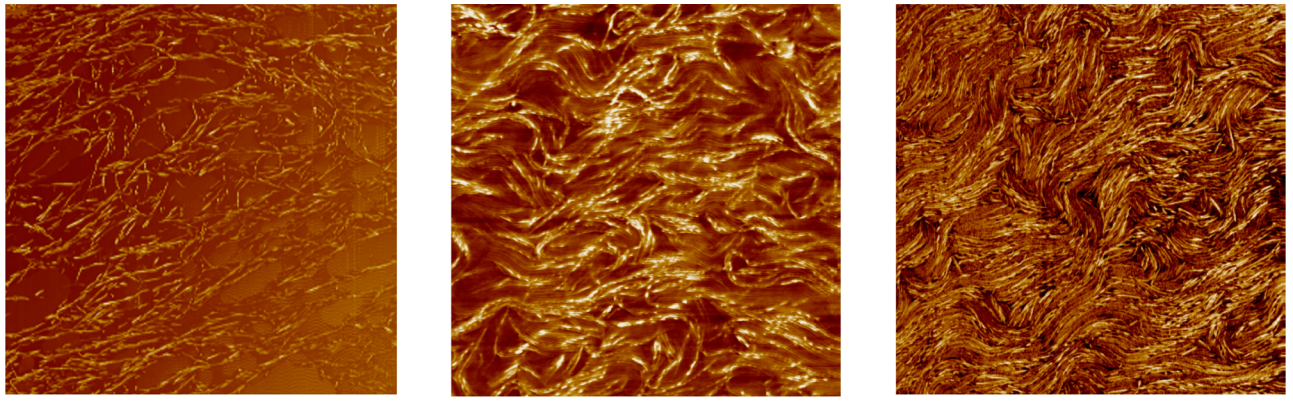

Figure 4. AFM micrographs (window size 10 μm) for selected HMDI-cross-linked lignocellulose gel-like dispersions: (a) GEK0; (b) GEK1; (c) GEK2.

degradation gases and a variety of hydrocarbon derivatives.[52] As depicted in Figure 2b, the nonmodified lignocellulose pulp sample starts to degrade later but reaches the maximum decomposition rate at lower temperature, around 260 °C. However, this thermal event is expanded for HMDI-modified lignocellulosic materials. Thus, T_{onset} was found at ~200 °C, but the maximum degradation rate was delayed up to 320 °C for EK2 sample. In fact, overlapped peaks in the range of 250 to 320 °C, corresponding to several fractions chemically modified to different extents, can be guessed for EK0.5 and EK1 samples, which indicates that the thermal stability of the cellulose skeleton was increased with HMDI modification. Obviously, the presence of substituents on the cellulose skeleton and the promotion of cross-linking are expected to influence thermal stability. The higher amount of coupling agent can induce a more regular rearrangement, thus forming a new ordered structure with improved thermal stability. A similar pattern was found by Huang[53] during the thermal degradation of cellulose tristearate. After the main thermal event, all samples gradually continue losing weight until reaching residues at 600 °C of 95% for EK0 and EK0.5, 93% for EK1 and 84% for EK2. During this process, the remaining compounds produce volatiles including combustible and noncombustible species at temperatures of around 350 °C. At higher temperatures, the degradation produces a smoldering phenomenon, leading to a slower mass loss.[54] The char residue of the EK2 sample is lower than that found in EK0, EK0.5, and EK1. Therefore, it seems clear that urethane segments degraded more easily producing volatiles.

AFM Analysis of HMDI-Cross-Linked Lignocellulose Pulp Gel-Like Dispersions. In contrast to classical microstructural observations carried out with transmission (TEM) and scanning (SEM) electron microscopy techniques, the main advantage of AFM is the observation of lubricating grease microstructure without needing to be modified, for instance by freezing or oil removing. Suitable microstructural characterization of nonwashed conventional lubricating grease was previously reported by just simply heating the sample at a temperature below the dropping point and then cooling down to room temperature in order to obtain a very smooth surface.[55] The same protocol was followed in this study. Figure 3a–c shows AFM micrographs for different oleogels prepared using HMDI-cross-linked lignocellulosic materials from different sources of origin and/or submitted to different pulping treatments (Kraft or semimechanical pulping). As can be observed, in all cases, rather long, twisted, and entangled fibers were found, which very much resemble the morphology of traditional lithium greases.[55] Slightly longer and especially axially twisted fibers were detected in the gel-like dispersions of *Pinus radiata* lignocellulose material (Figure 3a), whereas a more densely arranged fibrous structure was observed for lignocellulose obtained with a semimechanical pulping treatment (Figure 3c). On the contrary, larger hollow spaces among thicker fibers, apparently more swollen in the oil medium, were

DOI: 10.1021/acssuschemeng.5b00389
ACS Sustainable Chem. Eng. 2015, 3, 2130–2141

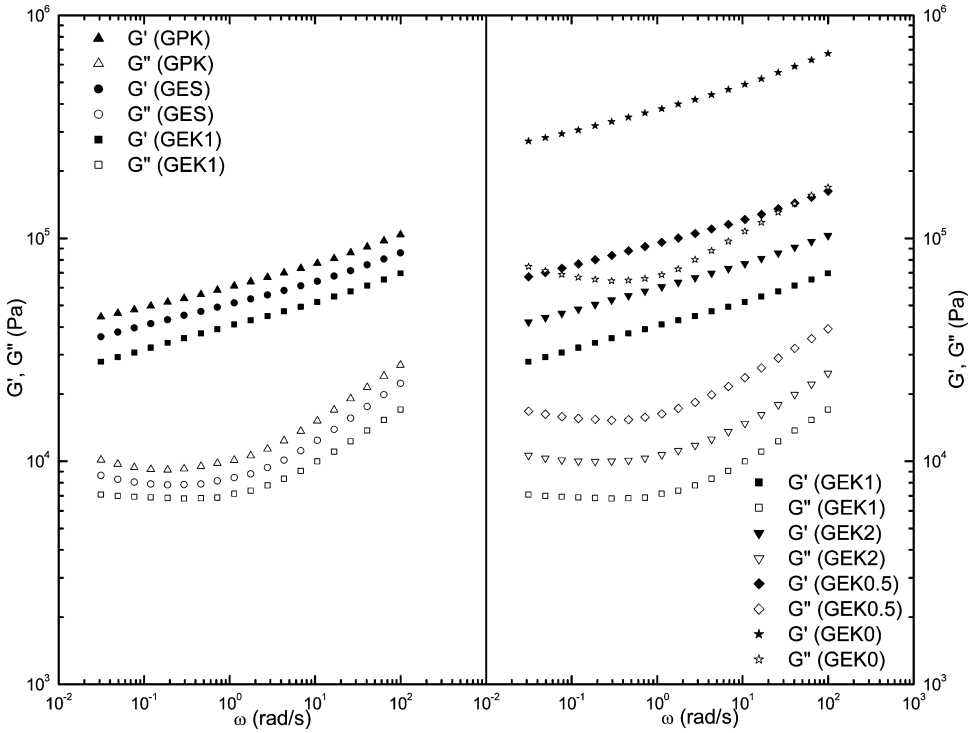

Figure 5. Frequency dependence of the storage, G', and loss, G'', moduli for the HMDI-cross-linked lignocellulose gel-like dispersions studied as a function of (a) source of origin of lignocellulose material and (b) HMDI/cellulose pulp weight ratio (G', closed symbols; G'', open symbols).

exhibited by the commercial grade Kraft *Eucaliptus globulus* lignocellulosic pulp gel-like dispersion (Figure 3b). These results can be explained attending to the polymerization degree of the original cellulosic pulps employed (see intrinsic viscosity data in Table 2).

The influence of HMDI/cellulose pulp weight ratio on oleogel morphology is shown in Figure 4. Clearly, the nonchemically modified lignocellulose material provides a dispersion of isolated and nonswollen solid particles randomly arranged in the oil medium (Figure 4a). More entangled and densely arranged fibers were obtained with HMDI-cross-linked lignocellulose. A particularly agglomerated fibrous structure was obtained when using a 2:1 HMDI/cellulose pulp weight ratio (Figure 4c).

Rheological Behavior of HMDI-Cross-Linked Lignocellulose Pulp Gel-Like Dispersions. Figure 5a shows the evolution of SAOS functions with frequency, at 25 °C, within the linear viscoelastic range for oleogels prepared with modified lignocellulose pulps obtained from different sources of origin and/or submitted to different pulping treatments. For the sake of comparison, this figure collects data corresponding to lignocellulosic pulps cross-linked with the same amount of coupling agent (HMDI). In all cases, the typical response of particle gels was obtained[56] wherein the so-called "plateau region" of the mechanical spectrum was clearly noticed. From a qualitative point of view, this response is very similar to that previously found in nonmodified cellulosic pulp/ethylcellulose blend dispersions[16,18] as well as in commercial lubricating greases based on mineral oils and metallic soaps.[55] As extensively investigated,[57−59] typically G' values in standard lithium lubricating greases of NLGI grades 1−3 range from 10^4 to 10^5 Pa, depending on composition and processing conditions, whereas G'' values are around 1 order of magnitude lower. Therefore, the HMDI-cross-linked lignocellulose pulp-based oleogels studied meet these requirements (Figure 5). The origin of lignocellulosic materials and the different pulping treatments do not significantly affect the values of the SAOS functions. In principle, the slight differences obtained could be related to the original fiber length and lignin and α-cellulose contents, as much more noticeably found for nonchemically modified cellulose pulp dispersions.[16] In any case, it seems clear that the cross-linking reaction significantly dampens this influence, although still slightly affecting the oleogel microstructure as previously discussed. On the contrary, as can be observed in Figure 5b, the amount of HMDI coupling agent added to the cross-linking reaction drastically influences the rheological behavior, although not in a trivial manner. Thus, the addition of a relatively small amount of HMDI (0.5:1 weight ratio) yields a drastic reduction in the values of the SAOS functions with respect to the non-cross-linked but mercerized cellulose pulp-based dispersion. In fact, the mercerized pulp dispersion in castor oil provides excessively high G' and G'' values to be proposed as a lubricating grease formulation. A further significant decrease in both moduli was again observed when applying a 1:1 HMDI/cellulose pulp weight ratio. However, a reverse effect was found when using an extensively cross-linked lignocellulosic material as the thickener agent (2:1 HMDI/cellulose pulp weight ratio), probably due to the highly packed and entangled structure achieved (see Figure 4c). Interestingly, the frequency dependence of SAOS functions and loss tangent values (relative elasticity) were not affected at all, and therefore, the amount of HMDI added to the cross-linking reaction may be simply used to modulate at convenience the values of the linear viscoelastic functions. This fact allows one to apply an empirical superposition method, using the plateau modulus, G_N^o, as a normalization factor. In this work, G_N^o was straightforwardly estimated as the G' value at a frequency for which the loss tangent is minimum.[60] Figure 6 shows the

DOI: 10.1021/acssuschemeng.5b00389
ACS Sustainable Chem. Eng. 2015, 3, 2130−2141

normalized master curve for G' and G'', as well as the evolution of G_N^o with the HMDI/cellulosic pulp ratio.

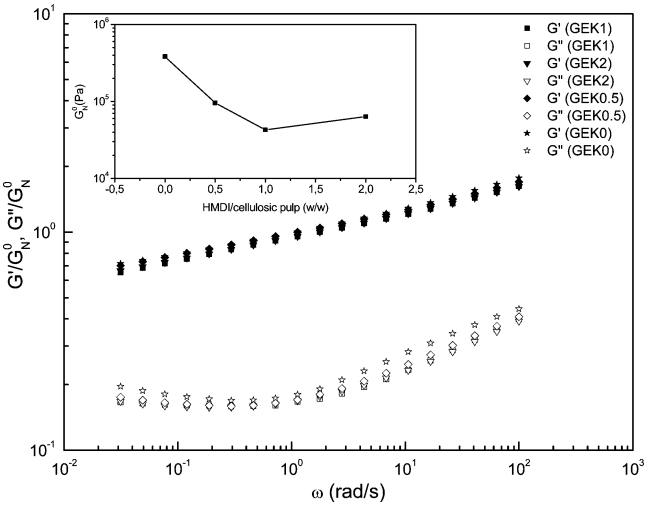

Figure 6. Normalized viscoelasticity functions and values of the plateau modulus as a function of the HMDI/cellulose pulp weight ratio. (G', closed symbols; G'', open symbols).

Regarding the thermo-rheological behavior, the temperature dependence of the SAOS functions is illustrated in Figure 7 for a selected sample. As can be seen, the linear viscoelastic functions, G' and G'', generally decrease with temperature (Figure 7a), much more sharply above 100 °C, associated with an increase in the loss tangent values, i.e., lower relative elasticity (Figure 7b). However, in all cases, a slight increase in the values of both G' and G'' were observed at 100 °C prior to the just mentioned dramatic decrease. Supported in the TGA analysis previously discussed, these effects must be attributed to the initial loss of structural water retained in lignocellulosic fibers at around 100 °C, yielding a more compact structure, and further disruption of urethane segments, which implies a reduction in the cross-linking degree, thus dramatically affecting the rheological response. The influence of temperature on linear viscoelasticy may be easily visualized and quantified by plotting the plateau modulus, G_N^o, versus the reciprocal temperature (Figure 8). As commented above, a sudden

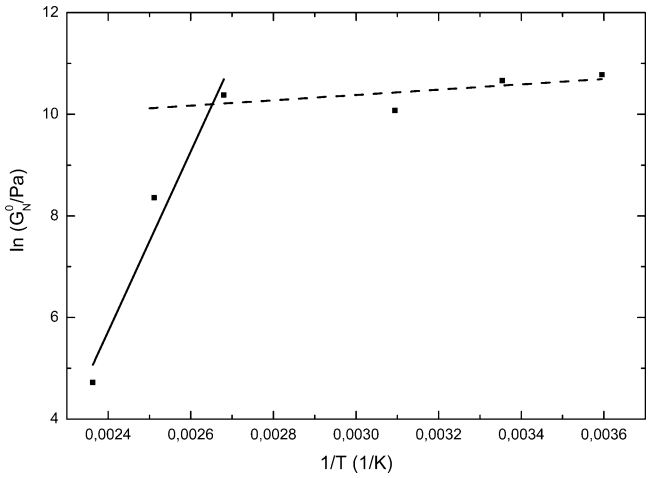

Figure 8. Evolution of the plateau modulus with temperature and Arrhenius' fitting (solid line) for sample GEK1.

change in the slope of G_N^o versus $1/T$ plot at around 100 °C was clearly detected, thus reflecting a much higher thermal

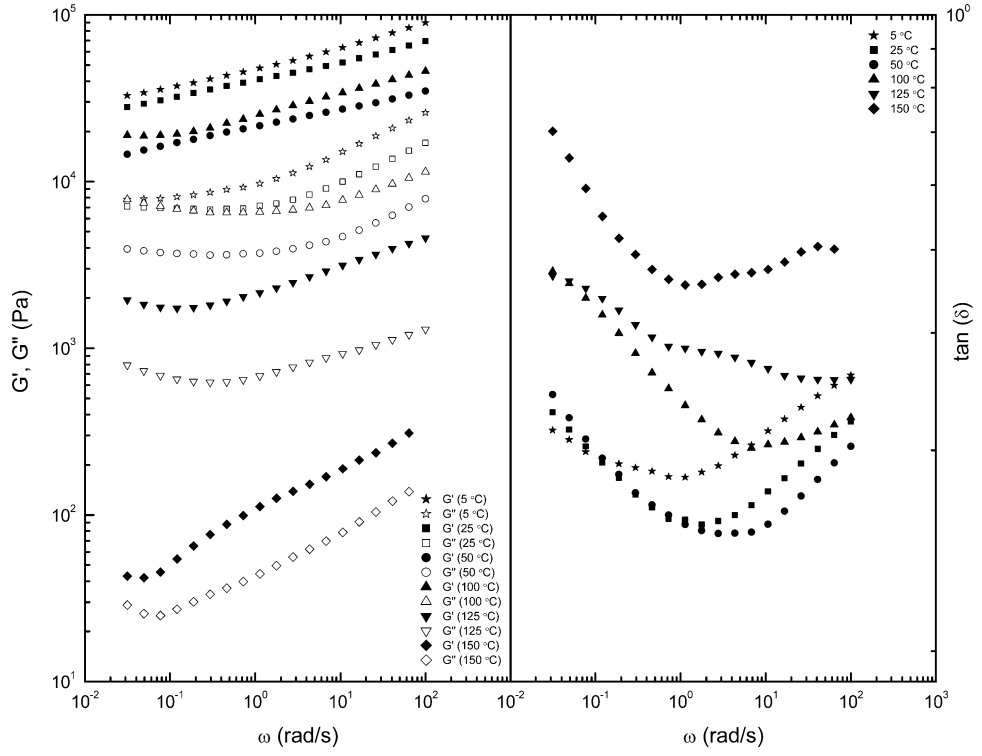

Figure 7. Evolution of (a) the storage, G', and loss, G'', moduli and (b) the loss tangent with the frequency at different temperatures for sample GEK1. (G, closed symbols; G'', open symbols).

DOI: 10.1021/acssuschemeng.5b00389
ACS Sustainable Chem. Eng. 2015, 3, 2130−2141

susceptibility of the oleogels studied at temperatures above this critical temperature. Two different Arrhenius-type relationships can be used to quantify the thermal dependence of the plateau modulus with temperature:

$$G_N^0 = A \cdot e^{E_a/R \cdot (\frac{1}{T})} \quad (1)$$

where E_a is a parameter which evaluates the thermal dependence, similar to the activation energy (J/mol), R is the gas constant (8.314 J/mol K), T is the absolute temperature (K), and A is the pre-exponential factor (Pa). Table 3 collects the values of E_a obtained from the fitting to eq 1 in both the low and high temperature ranges. In all samples studied, E_a values in the low temperature range are extremely low, which means a low thermal susceptibility, whereas much higher E_a values were obtained in the high temperature range. It is worth mentioning that very similar evolution was displayed by traditional metallic soap-based lubricating greases, where two different Arrhenius-type equations are also necessary to describe the thermo-rheological behavior.[61] The critical temperature reported for the change in thermal dependence in lithium greases was around 110 °C.

Table 3. Activation Energy Values, from eq 1 for the Different Gel-Like Dispersions Studied

	E_a (kJ/mol)	
sample	range 5 °C−100 °C	range 100 °C−150 °C
GPK	0.12	160.59
GES	−9.09	190.98
GEK1	4.36	147.39
GEK2	2.22	138.78
GEK0.5	2.02	128.61
GEK0	4.51	168.65

From a rheological point of view, the development of new grease formulations requires the characterization of both linear viscoelastic and viscous flow behaviors. It is well-known[44,61,62] that traditional lubricating greases exhibit different flow problems and shear-induced instabilities like wall-slip, shear banding, or fracture phenomena. Shear banding may be detected from the nonmonotonic evolution of the stress with shear rate obtained in controlled-shear rate rheometers, yielding a minimum in the flow curve, associated with a dynamically nonstable region at certain shear rate range,[63] which in lubricating greases is more apparent as temperature increases.[61] In this work, wall slip was overcome by using roughened plate−plate geometries, but on the contrary, such geometries favor the occurrence of fracture in the sample as a consequence of secondary flows.[64,65] Figure 9 shows the viscous flow curves in the form of apparent viscosity vs shear rate for the different lignocellulose pulp gel-like dispersions studied. As can be seen, no significant differences in viscosity were found for oleogels prepared with lignocellulosic materials of different origin (Figure 9a), whereas the amount of HMDI added to the cross-linking reaction affects the viscosity in the same direction than previously discussed for the linear viscoelastic functions (Figure 9b). Moreover, fracture was found to be evident for most of the samples at shear rates of around 10 s^{-1}, except for the non-cross-linked lignocellulose pulp which clearly evidences a fracture at 0.1 s^{-1}. This fact may be explained by attending to the lower hydrophobic interactions between this thickener and the base oil yielding a more fragile microstructure (see Figure 4a). Figure 10 shows the influence of temperature on the viscosity for a selected lignocellulose pulp dispersion. As can be seen, temperature significantly influences the values of viscosity,

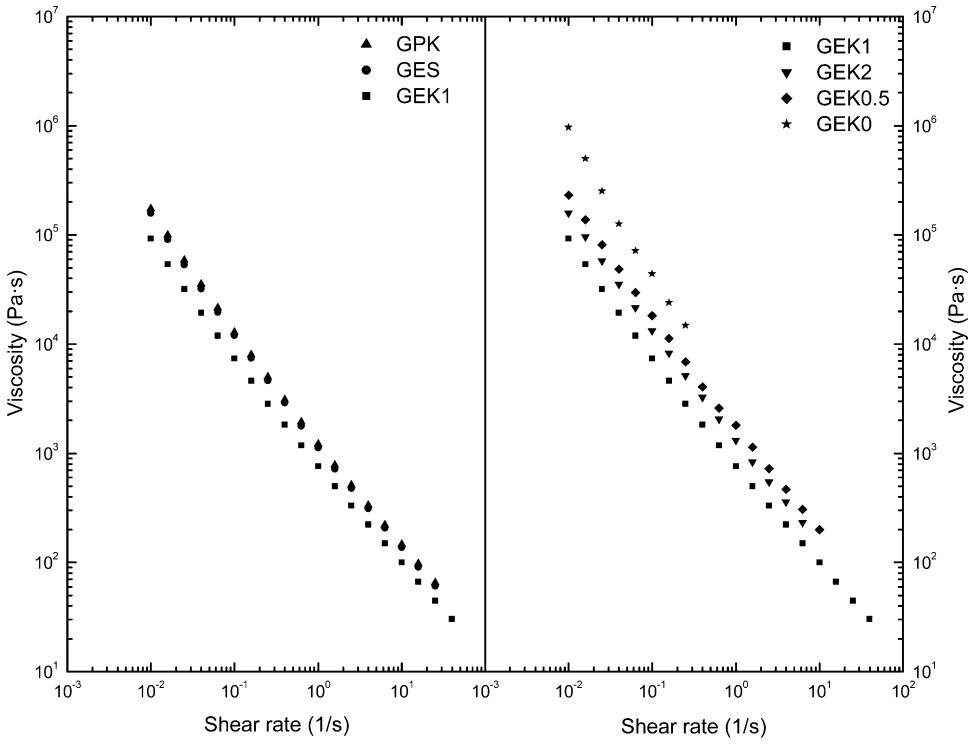

Figure 9. Viscous flow curves for the HMDI-cross-linked lignocellulose gel-like dispersions studied, at 25 °C, as a function of (a) source of origin of lignocellulose material and (b) HMDI/cellulose pulp weight ratio.

DOI: 10.1021/acssuschemeng.5b00389
ACS Sustainable Chem. Eng. 2015, 3, 2130−2141

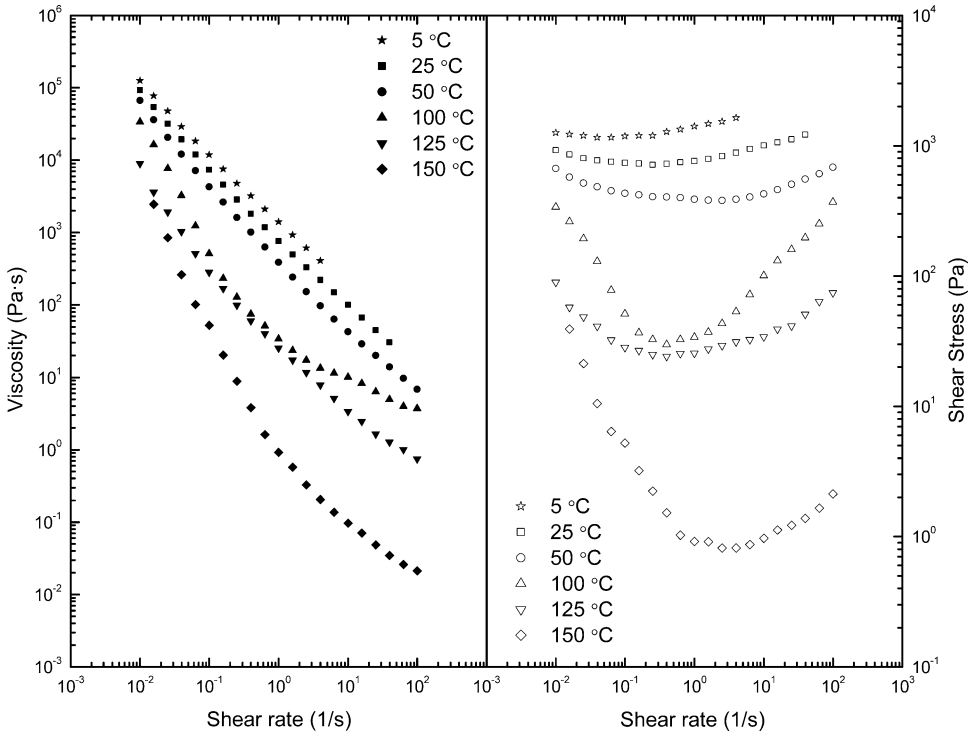

Figure 10. Influence of temperature on (a) shear rate dependence of viscosity and (b) evolution of the shear stress with shear rate for sample GEK1.

but more interestingly, as identically found in lubricating greases thickened with metallic soaps, temperature also favor the development of shear banding or nonhomogeneous flow, yielding a clear minimum in the evolution of the stress with shear rate above 50 °C (Figure 10b). This nonhomogeneity in the flow finally produces the macroscopic fracture of the sample, which in a lubricated contact may induce the expelling of the grease from the contact area but also a decrease in starvation due to oil bleeding.[66] In conclusion, the rheological behavior (viscous and viscoelastic) exhibited by HMDI-cross-linked lignocellulosic pulp gel-like dispersions in castor oil matches fairly well that required for lubricating greases, which can be otherwise quantitatively modulated by modifying the cross-linking degree of the lignocellulosic material used as thickening agent.

Lubrication Performance Properties of HMDI-Cross-Linked Lignocellulose Pulp Gel-Like Dispersions. Mechanical stability of lubricating greases is traditionally evaluated from the difference between penetration indexes obtained after and before submitting the sample to a standardized working test. Penetration of standard cone geometries inside a given grease sample is a common practice in the lubricant industry to determine grease consistency, which is obviously related to the rheological properties. Penetration values of 60 stroke worked samples (ASTM D217) are frequently used to classify lubricating greases in NLGI grades, according to the consistency degree, from extremely soft (grade 000) to highly consistent or solid-like (grade 6).[45] Table 4 shows the unworked penetration values of lignocellulose pulp gel-like dispersions studied. As may be seen, most of the samples show unworked penetration values between 190 and 250 mm/10, which would approximately correspond to NLGI grades 3−4, except that sample prepared with the nonchemically modified lignocellulosic pulp which presents the highest consistency, in agreement with the rheological response previously discussed.

Table 4. Penetration and Mechanical Roll Stability Values for the Different Gel-Like Dispersions Studied

sample	unworked penetration (mm/10)	worked penetration (mm/10)	penetration variation (mm/10)
GPK	204	215	11
GES	204	208	4
GEK0	115	112	−3
GEK0.5	192	196	4
GEK1	252	263	11
GEK2	208	218	10

Besides this, mechanical stability was determined after performing the standard rolling test which applies severe shear conditions. In principle, greases with good mechanical stability must exhibit penetration increments after working below 10−15 mm/10 and as close to zero as possible. Table 4 also collects the penetration values obtained after working the sample and corresponding penetration increments. The lack of physical and mechanical stabilities of nonchemically treated cellulosic pulp-based dispersions previously studied was the main adverse factor to consider those formulations as efficient alternatives to lubricating greases, generally showing increments of penetrations higher than 30 mm/10.[16] However, all the oleogels based on HMDI-cross-linked lignocellulosic materials present acceptable mechanical stability values (Table 4). The negative increment of penetration shown by the nonchemically modified lignocellulose pulp-based dispersion can be explained attending to its high consistency and poor physical stability, which promotes a significant oil separation especially after the application of a severe shearing treatment, thus increasing the effective thickener concentration.

The potential applicability of these HMDI-cross-linked lignocellulose pulp-based oleogels was also investigated in a ball-on-plate tribological contact. Specific normal load (20 N)

DOI: 10.1021/acssuschemeng.5b00389
ACS Sustainable Chem. Eng. 2015, 3, 2130−2141

and rotational speed (10 rpm) conditions were selected to achieve the mixed lubrication regime, previously determined by performing ramps of rotational speed, i.e., the Stribeck curves.[67] Table 5 includes the steady-state values of the friction coefficients obtained under these conditions and the average diameter of the resulting wear marks found in the bottom steel plates. The same parameters were also evaluated for two commercial lubricating greases, a traditional lithium lubricating grease and a semibiodegradable calcium grease containing a vegetable oil as base oil. As can be observed, reasonable low friction coefficient values were obtained for most of the cellulosic pulp dispersions analyzed but higher than those obtained with the commercial lubricants. However, this fact must be in part attributed to the lower consistency of commercial lubricating greases. As previously reported,[68] the friction coefficient generally increases with NLGI grade. Particularly high friction coefficient values were obtained for oleogels prepared with the nonchemically modified lignocellulose pulp and that containing the modified *Pinus radiata* lignocellulose pulp. On the contrary, wear mark diameters were in most cases comparable to that obtained with the calcium grease, although still higher than that produced when using the lithium grease as lubricant. In this case, particularly large wear marks were obtained when using either a high proportion of coupling agent or the chemically modified pine Kraft lignocellulose pulp. In this sense, it is worth mentioning that friction and wear analysis always depend on each other in the total frictional system and that sometimes friction is simply reduced as a consequence of increasing wear. This could be the case of the formulation thickened with a highly HMDI-cross-linked ligocellulosic pulp.

Table 5. Friction Coefficient Values and Average Diameter of Wear Marks on Plates Obtained in a Ball-on-Plates Configuration When Using the HMDI-Cross-Linked Lignocellulose Gel-Like Dispersions and Standard Lubricating Greases as Lubricants

Sample	friction coefficient	wear mark diameter (μm)
GPK	0.147 ± 0.007	409
GES	0.133 ± 0.001	372
GEK0	0.149 ± 0.003	301
GEK0.5	0.136 ± 0.008	358
GEK1	0.129 ± 0.004	331
GEK2	0.124 ± 0.009	481
commercial lithium grease	0.110 ± 0.002	273
commercial calcium grease	0.106 ± 0.004	321

CONCLUSIONS

Several lignocellulosic materials from different sources of origin and/or submitted to different pulping treatments were chemically modified by performing a cross-linking reaction, using HMDI as the coupling agent, and further dispersed in castor oil in order to analyze their thickening ability in this medium. In general, the HMDI-cross-linked lignocellulose gel-like dispersions attained fit the rheological and tribological property requirements as well as suitable physical and mechanical stabilities to be proposed as efficient biodegradable alternatives to traditional lubricating greases. In particular, both the thermo-rheological response, which evidences a softening temperature of around 100 °C, and the microstructural morphology, composed of long and entangled fibers, are extremely similar to those found in lithium greases. The mechanical stability of HMDI-cross-linked lignocellulose-based oleogels, evaluated as the loss of consistency after submitting the sample to a working test, was significantly improved with respect to the non-cross-linked lignocellulose gel-like dispersions previously studied. Moreover, the friction coefficient and resulting wear mark diameters obtained in a ball-on-disc contact lubricated with these eco-friendly formulations were, in most cases, comparable to that obtained with commercial lubricating greases.

The HMDI/cellulose pulp weight ratio applied in the cross-linking reaction can be used to modify and modulate the consistency and the values of rheological functions and parameters of these gel-like dispersions. However, the rheological behavior is not qualitatively affected by the amount of HMDI used as coupling agent, which allows one to obtain master curves of the SAOS functions by applying an empirical superposition method, using the plateau modulus, G_N^o, as a normalization factor.

Therefore, HMDI-cross-linked lignocellulosic materials can be introduced as effective and promising eco-friendly thickener agents in vegetable oil-derived base oils resulting in lubricating grease formulations completely based on renewable resources.

AUTHOR INFORMATION

Corresponding Author

*Phone: +34959219995. Fax: +34959219983. E-mail: franco@uhu.es.

Notes

The authors declare no competing financial interest.

ACKNOWLEDGMENTS

This work is a part of two research projects (CTQ2014-56038-C3-1R and TEP-1499) sponsored by the MINECO-FEDER and Junta de Andalucía programmes, respectively. R.G. has received a Ph.D. Research Grant (BES-2011-045029) from DIGICyT (MINECO). The authors gratefully acknowledge the financial support.

REFERENCES

(1) Octave, S.; Thomas, D. Biorefinery: Toward an industrial metabolism. *Biochimie* **2009**, *91*, 659−664.
(2) Wilson, B. Lubricants and functional fluids from renewable sources. *Ind. Lubr. Tribol.* **1998**, *50*, 6−15.
(3) Boyde, S. Green lubricants. Environmental benefits and impacts of lubrication. *Green Chem.* **2002**, *4*, 293−307.
(4) Salimon, J.; Salih, N.; Yousuf, E. Biolubricants: raw materials, chemical modifications and environmental benefits. *Eur. J. Lipid Sci. Technol.* **2010**, *112*, 519−530.
(5) Garcés, R.; Martínez-Force, E.; Salas, J. J. Vegetable oil basestocks for lubricants. *Grasas Aceites* **2011**, *62*, 21−28.
(6) Quinchia, L. A.; Delgado, M. A.; Valencia, C.; Franco, J. M.; Gallegos, C. Viscosity modification of different vegetable oils with EVA copolymer for lubricant applications. *Ind. Crops Prod.* **2010**, *32*, 607−612.
(7) Quinchia, L. A.; Delgado, M. A.; Franco, J. M.; Spikes, H. A.; Gallegos, C. Low-temperature flow behaviour of vegetable oil-based lubricants. *Ind. Crops Prod.* **2012**, *37*, 383−388.
(8) Asadauskas, S.; Perez, J. M.; Duda, J. L. Lubrication properties of castor oil - Potential basestock for biodegradable lubricants. *Lubr. Eng.* **1997**, *53*, 35−41.
(9) Maleque, M.; Masjuki, H.; Sapuan, S. Vegetable-based biodegradable lubricating oil additives. *Ind. Lubr. Tribol.* **2003**, *55*, 137−143.

DOI: 10.1021/acssuschemeng.5b00389
ACS Sustainable Chem. Eng. 2015, 3, 2130−2141

(10) Karmakar, G.; Ghosh, P. Green additives for lubricating oil. *ACS Sustainable Chem. Eng.* **2013**, *1*, 1364−1370.
(11) Karmakar, G.; Ghosh, P. Soybean oil as a biocompatible multifunctional additive for lubricating oil. *ACS Sustainable Chem. Eng.* **2015**, *3*, 19−25.
(12) Li, W.; Jiang, C.; Chao, M.; Wang, X. Natural garlic oil as a high-performance, environmentally friendly, extreme pressure additive in lubricating oils. *ACS Sustainable Chem. Eng.* **2014**, *2*, 798−803.
(13) Singh, R. K.; Kukrety, A.; Singh, A. K. Study of novel ecofriendly multifunctional lube additives based on pentaerythritol phenolic ester. *ACS Sustainable Chem. Eng.* **2014**, *2*, 1959−1967.
(14) Singh, R. K.; Kukrety, A.; Chatterjee, A. K.; Thakre, G. D.; Bahuguna, G. M.; Saran, S.; Adhikari, D. K.; Atray, N. Use of an acylated chitosan schiff base as an ecofriendly multifunctional biolubricant additive. *Ind. Eng. Chem. Res.* **2014**, *53*, 18370−18379.
(15) Singh, R. K.; Singh, A. K. Abilities of some compounds to stabilize mahwa oil from high temperature oxidative degradation for biolubricant applications. *Waste Biomass Valorization* **2014**, *5*, 847−855.
(16) Nuñez, N.; Martin-Alfonso, J. E.; Eugenio, M. E.; Valencia, C.; Diaz, M. J.; Franco, J. M. Preparation and characterization of gel-like dispersions based on cellulosic pulps and castor oil for lubricant applications. *Ind. Eng. Chem. Res.* **2011**, *50*, 5618−5627.
(17) Nuñez, N.; Martin-Alfonso, J. E.; Valencia, C.; Sanchez, M. C.; Franco, J. M. Rheology of new green lubricating grease formulations containing cellulose pulp and its methylated derivative as thickener agents. *Ind. Crops Prod.* **2012**, *37*, 500−507.
(18) Martin-Alfonso, J. E.; Nuñez, N.; Valencia, C.; Franco, J. M.; Diaz, M. J. Formulation of new biodegradable lubricating greases using ethylated cellulose pulp as thickener agent. *J. Ind. Eng. Chem.* **2011**, *17*, 818−823.
(19) Satyanarayana, K. G.; Arizaga, G. G. C.; Wypych, F. Biodegradable composites based on lignocellulosic fibers − an overview. *Prog. Polym. Sci.* **2009**, *34*, 982−1021.
(20) Dufresne, A.; Belgacem, M. N. Cellulose-reinforced composites: from micro to nanoscale. *Polimeros* **2013**, *23*, 277−286.
(21) Satyanarayana, K. G. Steam explosion − a boon for value addition to renewal resources. *Metal News* **2004**, *22*, 35−40.
(22) Lopez, J. P.; Mutje, P.; Pelach, M. A.; El Mansouri, N. E.; Boufi, S.; Vilaseca, F. Analysis of the tensile modulus of polypropylene composites reinforced with stone groundwood fibers. *Bioresources* **2012**, *7*, 1310−1323.
(23) Montano-Leyva, B.; da Silva, G. G. D.; Gastaldi, E.; Torres-Chavez, P.; Gontard, N.; Angellier-Coussy, H. Biocomposites from wheat proteins and fibers: Structure/mechanical properties relationships. *Ind. Crops Prod.* **2013**, *43*, 545−555.
(24) Parparita, E.; Darie, R. N.; Popescu, C. M.; Uddin, M. A.; Vasile, C. Structure-morphology-mechanical properties relationship of some polypropylene/lignocellulosic composites. *Mater. Eng.* **2014**, *56*, 763−772.
(25) Aydemir, D.; Kiziltas, A.; Kiziltas, E. E.; Gardner, D. J.; Gunduz, G. Heat treated wood-nylon 6 composites. *Composites, Part B* **2015**, *68*, 414−423.
(26) Gulati, I.; Park, J.; Maken, S.; Lee, M. G. Production of carboxymethylcellulose fibers from waste lignocellulosic sawdust using $NaOH/NaClO_2$ pretreatment. *Fibers Polym.* **2014**, *15*, 680−686.
(27) Samaniuk, J. R.; Scott, C. T.; Root, T. W.; Klingenberg, D. J. Rheological modification of corn stover biomass at high solids concentrations. *J. Rheol.* **2012**, *56*, 649−665.
(28) Hu, S. J.; Luo, X. L.; Li, Y. B. Polyols and polyurethanes from the liquefaction of lignocellulosic biomass. *ChemSusChem* **2014**, *7*, 66−72.
(29) Xu, J. M.; Jiang, J. C.; Hse, C. Y.; Shupe, T. F. Preparation of polyurethane foams using fractionated products in liquefied wood. *J. Appl. Polym. Sci.* **2014**, *131*, 40096.
(30) Yang, R.; Wang, Y.; Li, M. Homogeneous synthesis of crosslinked cellulose spheres from hemp (Cannabis sativa l.) stem and cotton. *Cell. Chem. Technol.* **2014**, *48*, 455−459.
(31) Luo, X. G.; Mohanty, A.; Misra, M. Lignin as a reactive reinforcing filler for water-blown rigid biofoam composites from soy oil-based polyurethane. *Ind. Crops Prod.* **2013**, *47*, 13−19.
(32) Gao, Z. H.; Ma, D. Y.; Lv, X. Y.; Zhang, Y. H. Effects of vinyl isocyanate coupling agent on the tensile properties of Kraft fiber-unsaturated polyester composites. *J. Appl. Polym. Sci.* **2013**, *128*, 1036−1043.
(33) Girones, J.; Pimenta, M. T. B.; Carvalho, A. J. F.; Mutje, P.; Curvelo, A. A. S. Blocked diisocyanates as reactive coupling agents: Application to pine fiber-polypropylene composites. *Carbohydr. Polym.* **2008**, *74*, 106−113.
(34) Girones, J.; Pimenta, M. T. B.; Vilaseca, F.; de Carvalho, A. J. F.; Mutje, P.; Curvelo, A. A. S. Blocked isocyanates as coupling agents for cellulose-based composites. *Carbohydr. Polym.* **2007**, *68*, 537−543.
(35) Tonoli, G. H. D.; Mendes, R. F.; Siqueira, G.; Bras, J.; Belgacem, M. N.; Savastano, H. Isocyanate-treated cellulose pulp and its effect on the alkali resistance and performance of fiber cement composites. *Holzforschung* **2013**, *67*, 853−861.
(36) Shang, W. L.; Huang, J.; Luo, H.; Chang, P. R.; Feng, J. W.; Xie, G. Y. Hydrophobic modification of cellulose nanocrystal via covalently grafting of castor oil. *Cellulose* **2013**, *20*, 179−190.
(37) Qiu, X. Y.; Tao, S. M.; Ren, X. Q.; Hu, S. W. Modified cellulose films with controlled permeatability and biodegradability by cross-linking with toluene diisocyanate under homogeneous conditions. *Carbohydr. Polym.* **2012**, *88*, 1272−1280.
(38) Siqueira, G.; Bras, J.; Dufresne, A. New process of chemical grafting of cellulose nanoparticles with a long chain isocyanate. *Langmuir* **2010**, *26*, 402−411.
(39) Rials, T. G.; Wolcott, M. P.; Nassar, J. M. Interfacial contributions in lignocellulosic fiber-reinforced polyurethane composites. *J. Appl. Polym. Sci.* **2001**, *80*, 546−555.
(40) Yu, C. S.; Liu, H. P.; Li, Y. Q.; Zu, Y. G. Preparation and characterization of degradable cellulose-based macroporous resin. *Polym. Int.* **2012**, *61*, 994−1001.
(41) Fischer, F.; Rigacci, A.; Pirard, R.; Berthon-Fabry, S.; Achard, P. Cellulose-based aerogels. *Polymer* **2006**, *47*, 7636−7645.
(42) Gallego, R.; Arteaga, J. F.; Valencia, C.; Franco, J. M. Rheology and thermal degradation of isocyanate-functionalized methyl cellulose-based oleogels. *Carbohydr. Polym.* **2013**, *98*, 152−160.
(43) Wise, L. E.; Murphy, M.; D'Adieco, A. Chlorite holocellulose, its fractionation and beating on summative wood analysis and on studies on the hemicellulose. *Technol. Assoc. Pap.* **1946**, *29*, 210.
(44) Balan, C.; Franco, J. M. Influence of the geometry on the transient and steady flow of lubricating greases. *Tribol. Trans.* **2001**, *44*, 53−58.
(45) NLGI. *Lubricating Greases Guide*; National Lubricating Grease Institute: Kansas City, MO, 2006.
(46) Sgriccia, N.; Hawley, M.; Misra, M. Characterization of natural fiber surfaces and natural fiber composites. *Composites, Part A* **2008**, *39*, 1632−1637.
(47) Sekiguchi, Y.; Sawatari, C.; Kondo, T. A. A gelation mechanism depending on hydrogen bond formation in regioselectively substituted O-methylcelluloses. *Carbohydr. Polym.* **2003**, *53*, 145−153.
(48) Baiardo, M.; Frisoni, G.; Scandola, M.; Licciardello, A. Surface chemical modification of natural cellulose fibers. *J. Appl. Polym. Sci.* **2002**, *83*, 38−45.
(49) Ciolacu, D.; Ciolacu, F.; Popa, V. I. Amorphous cellulose-Structure and characterization. *Cellul. Chem. Technol.* **2011**, *45*, 13−21.
(50) Scheirs, J.; Camino, G.; Tumiatti, W. Overview of water evolution during the thermal degradation of cellulose. *Eur. Polym. J.* **2001**, *37*, 933−942.
(51) Poletto, M.; Pistor, V.; Zattera, A. J. Structural Characteristics and Thermal Properties of Native Cellulose. In *Cellulose - Fundamental Aspects*; Van de Ven, T., Godbout, L., Eds.; InTech: Rijeka, Croatia, 2013.
(52) Bourbigot, S.; Chlebicki, S.; Mamleev, V. Thermal degradation of cotton under linear heating. *Polym. Degrad. Stab.* **2002**, *78*, 57−62.
(53) Huang, F. Y. Thermal properties and thermal degradation of cellulose tri-stearate (CTs). *Polymers* **2012**, *4*, 1012−1024.

DOI: 10.1021/acssuschemeng.5b00389
ACS Sustainable Chem. Eng. 2015, 3, 2130−2141

(54) Chen, Y.; Frendi, A.; Tewari, S. S.; Sibulkin, M. Combustion properties of pure and fire-retarded cellulose. *Combust. Flame* **1991**, *84*, 121−140.
(55) Sanchez, M. C.; Franco, J. M.; Valencia, C.; Gallegos, C.; Urquiola, F.; Urchegui, R. Atomic force microscopy and thermo-rheological characterization of lubricating greases. *Tribol. Lett.* **2011**, *41*, 463−470.
(56) Almdal, K.; Dyre, J.; Hvidt, S.; Kramer, O. Towards a phenomenological definition of the term "gel. *Polym. Gels Networks* **1993**, *1*, 5−17.
(57) Franco, J. M.; Delgado, M. A.; Valencia, C.; Sánchez, M. C.; Gallegos, C. Mixing rheometry for studying the manufacture of lubricating greases. *Chem. Eng. Sci.* **2005**, *60*, 2409−2418.
(58) Delgado, M. A.; Valencia, C.; Sánchez, M. C.; Franco, J. M.; Gallegos, C. Influence of soap concentration and oil viscosity on the rheology and microstructure of lubricating greases. *Ind. Eng. Chem. Res.* **2006**, *45*, 1902−1910.
(59) Martin-Alfonso, J. E.; Valencia, C.; Sánchez, M. C.; Franco, J. M.; Gallegos, C. Rheological modification of lubricating greases with recycled polymers from different plastic waste. *Ind. Eng. Chem. Res.* **2009**, *48*, 4136−4144.
(60) Liu, C. Y.; He, J. S.; Van Ruymbeke, E.; Keunings, R.; Bailly, C. Evaluation of different methods for the determination of the plateau modulus and the entanglement molecular weight. *Polymer* **2006**, *47*, 4461−4479.
(61) Delgado, M. A.; Valencia, C.; Sanchez, M. C.; Franco, J. M.; Gallegos, C. Thermorheological behaviour of a lithium lubricating grease. *Tribol. Lett.* **2006**, *23*, 47−54.
(62) Martin-Alfonso, J. E.; Valencia, C.; Sanchez, M. C.; Franco, J. M. The effect of recycled polymer addition on the thermorheological behavior of modified lubricating greases. *Polym. Eng. Sci.* **2013**, *53*, 818−826.
(63) Coussot, P.; Lenov, A. I.; Piau, J. M. Rheology of concentrated dispersed systems in a low-molecular-weight matrix. *J. Non-Newtonian Fluid Mech.* **1993**, *46*, 179−217.
(64) Hutton, J. F. Using Weissenberg rheogoniometer to measure normal stresses in lubricating greases as examples of materials which have a yield stress. *Rheol. Acta* **1975**, *14*, 979−992.
(65) Chang, G. S.; Koo, J. S.; Song, K. W. Wall slip of vaseline in steady shear rheometry. *Korean-Aust. Rheol. J.* **2003**, *15*, 55−61.
(66) Larsson, P. O.; Jacobson, B.; Hoglund, E. Oil drops leaving an EHD contact. *Wear* **1994**, *179*, 23−28.
(67) Burstein, L. Lubrication and Roughness. In *Tribology for Engineers: A Practical Guide*; Davim, J. P., Ed.; Woodhead Publishing, Cambridge, 2011.
(68) Martin-Alfonso, J. E.; Romero, A.; Valencia, C.; Franco, J. M. Formulation and processing of virgin and recycled polyolefin/oil blends for the development of lubricating greases. *J. Ind. Eng. Chem.* **2013**, *19*, 580−588.

DOI: 10.1021/acssuschemeng.5b00389
ACS Sustainable Chem. Eng. 2015, 3, 2130−2141